13. A. T. Onufriev and S. A. Kristianovich, "Features of turbulent motion in a vortex ring," Dokl. Akad. Nauk SSSR, 229, No. 1, 42-44 (1976).
14. A. T. Onufriev, "Phenomenological models of turbulence," in: Aerodynamics and Physical Kinetics. Tr. Inst. Teor. Prikl. Mekh. Sib. Otd. Akad. Nauk SSSR, Novosibirsk (1977), pp. 43-66.
15. L. A. Vulis and V. P. Kashkarov, Theory of a Jet of a Viscous Fluid [in Russian], Nauka, Moscow (1965).
16. V. S. Krylov, "Diffusion boundary layer on the surface of a moving drop in the presence of a bulk chemical reaction," Izv. Akad. Nauk SSSR, Mekh. Zhidk. Gaza, No. 1, 146-149 (1967).
17. V. G. Levich, Physicochemical Hydrodynamics, Prentice-Hall (1972).
18. R. Mises, "Bermerkungen zur Hydrodynamik," Z. Angew. Math. Mech., 7, 425-431 (1927).
19. A. N. Tikhonov and A. A. Samarskii, Equations of Mathematical Physics [in Russian], Nauka, Moscow.
20. D. W. Moore, "The velocity of rise of distorted gas bubbles in a liquid of small velocity," J. Fluid Mech., 23, Pt. 4, 749-766 (1965).

MODIFIED BOUNDARY CONDITIONS FOR TWO-DIMENSIONAL GASDYNAMIC CALCULATIONS IN REGIONS OF ARBITRARY SHAPE WITH MOVING BOUNDARIES PRESENT

G. S. Romanov and V. V. Urban

UDC 533.6

Boundary conditions enabling one to improve the accuracy, convergence, and economy on numerical calculations are discussed.

Numerical calculations of gasdynamic flows in regions with arbitrary curved boundaries are greatly complicated by the difficulties of constructing the finite-difference grid (coordinate system) and approximating the boundary conditions. Because of this, much interest has recently been devoted to the investigation of ways of generating coordinate systems, accomplished, e.g., using conformal and quasiconformal transformations, elliptic equations, and algebraic transformations [1, 2]. Several ways of automating the distribution of the coordinate lines and monitoring them have been determined and a theoretical study of the errors introduced into the solution by arbitrary coordinate systems has begun. Nevertheless, the construction of a "good" coordinate system in regions of arbitrary shape where the boundary conditions are easily assigned is still a difficult problem of independent importance. Therefore, the search for ways of using simpler procedures to describe curved boundaries and assign boundary conditions is timely.

Below we consider a method of calculating boundary cells obtained by superposing an irregular orthogonal grid onto boundaries of arbitrary shape, already proposed in the period of the first computer calculations, according to [3]. Detailed information about this so-called method of fractional cells is contained in [4], where the necessary calculating equations are given. Work is known in which modified boundary conditions were introduced within the framework of the method of fractional cells. Thus, in [5] a moving undeformed boundary, a piston, is introduced along one of the coordinate axes, and the number of types of fractional cells is reduced to two using an irregular orthogonal grid. A more universal method of calculating curved boundaries moving arbitrarily over a grid was proposed in [6]. In this case conservative equations for boundary purposes and fractional cells are used in [5, 6]. In [5, 7] the condition of nonpenetration at the fixed curved boundaries is supplemented by the condition of stream slippage, realized through reorganization of the velocity vector in the fractional cells.

The aim of the present work is to clarify the role of the boundary conditions at curved

V. I. Lenin Belorussian State University, Minsk. Translated from Inzhenerno-Fizicheskii Zhurnal, Vol. 50, No. 1, pp. 40-48, January, 1986. Original article submitted September 24, 1984.

 0022-0841/86/5001-0030$12.50

and moving boundaries, on the example of two-dimensional gasdynamic problems through test calculations made by the method of large particles [4], in the improvement of the accuracy, convergence, and economy of the computational process. Since the given conditions require a partial change in the finite-difference equations in the boundary cells, we first consider the statement of these conditions and then we write the entire system of equations.

In a region D let there be a curved surface Γ approximated by segments of straight lines connecting the points of intersection of its contour with the lines of an irregular orthogonal grid. It is assumed that the sequence of points of intersection G(k), k = 1, 2, ..., K, is numbered and that the circuit is made counterclockwise, i.e., so that the body lies to the left of the boundary. In the general case 12 types of fractional cells are possible (Fig. 1a). Let us consider the statement of the boundary conditions in the fractional cell shown in Fig. 1b. The standard procedure for calculating such a cell [4] consists in assigning conditions of nonpenetration on the side z_{k+1} (the velocity is assumed to equal zero at it) and of partial penetration on the sides r_k and r_{k+1}. The latter differs from the case on the size z_k (free inflow—outflow) only by a decrease in the flows r_k and r_{k+1} in proportion to their sizes (e.g., the areas of the boundaries). Leaving the rules of calculation of fractional cells in force, we introduce the additional condition of stream slippage along the boundary $\Gamma\Gamma$ by analogy with [5, 7]. Let the components of the velocity vector w be determined at the geometrical center; then, introducing the local Cartesian coordinate system ξ, τ at this point, we can exactly assign the condition of stream slippage, reconstructing the vector $\mathbf{w} \to \mathbf{w}'$ so that its component w_ξ normal to the surface of the boundary $\Gamma\Gamma$ is reduced to zero (Fig. 1b). The new values of the components of the velocity vector will be defined by the expressions

$$v'_{ij} = (u_{ij}\Delta_{ij} + v_{ij})/(1 + \Delta_{ij}^2), \quad u'_{ij} = v'_{ij}\Delta_{ij}, \tag{1}$$

where $\Delta_{ij} = (z_{k+1} - z_k)\,\Delta z_i/(r_{k+1} - r_k)\,\Delta r_j$, $0 \leqslant z_k \leqslant 1$, $0 \leqslant r_k \leqslant 1$, k = 1, 2, 3, ..., K. Obviously, the condition (1) is not universal and is suitable for acceleration of the process of establishment in flow over stationary boundaries. For a moving boundary the velocity vector in an adjacent cell can have an arbitrary direction. In this case the velocities of the gas and the boundary are usually taken as equal, and the velocity of motion of the latter can be determined using additional equations.

Let the velocity of the boundary be determined and equal to U. Then in a time Δt, in moving into the cell, an element of the boundary moves a mass $\Delta M = \rho S U \Delta t$ and increases the energy of the gas by an amount $\Delta E = p\Delta V$. It is proposed to modify the increment in energy by setting it equal to

$$\Delta E = \rho U \Delta t\,(E + E_*)\,S, \tag{2}$$

where $E_* = (U^2 - u^2)0.5$ is the difference between the specific kinetic energies of the piston and of the gas displaced by it. Equation (2) contains the auxiliary term E_*, which should help to equate the velocities of the boundary and of the contiguous gas through the input (during acceleration) or the output (during deceleration) of a certain amount of kinetic energy. Obviously, one must require that the energy unbalance be as minimal as possible and not make a decisive contribution to the energetics of the specific problem. With allowance for (1)-(2) we write the system of finite-difference equations of the method of large particles for irregular grid steps and arbitrary cells.

First stage:

$$\begin{gathered}
u_{ij} = u_{ij}^n - A\,[S_{i+1/2}\,(p_{i+1,j}^n - p_{ij}^n) + S_{i-1/2}\,(p_{ij}^n - p_{i-1,j}^n)], \\
v_{ij} = v_{ij}^n - A\,[S_{j+1/2}\,(p_{i,j+1}^n - p_{ij}^n) + S_{j-1/2}\,(p_{ij}^n - p_{i,j-1}^n)], \\
\tilde{E}_{ij}^n = E_{ij}^n - 2A\,[S_{i+1/2}p_{i+1/2,j}^n\,u_{i+1/2,j}^n - S_{i-1/2}p_{i-1/2,j}^n\,u_{i-1/2,j}^n + \\
+ S_{j+1/2}p_{i,j+1/2}^n\,v_{i,j+1/2}^n - S_{j-1/2}p_{i,j-1/2}^n\,v_{i,j-1/2}^n].
\end{gathered} \tag{3}$$

In the whole cells $\tilde{u}_{ij}^n = u_{ij}$ and $\tilde{v}_{ij}^n = v_{ij}$, while in the fractional cells $\tilde{u}_{ij}^n$ and $\tilde{v}_{ij}^n$ are determined through u_{ij} and v_{ij} from Eqs. (1).

Second stage:

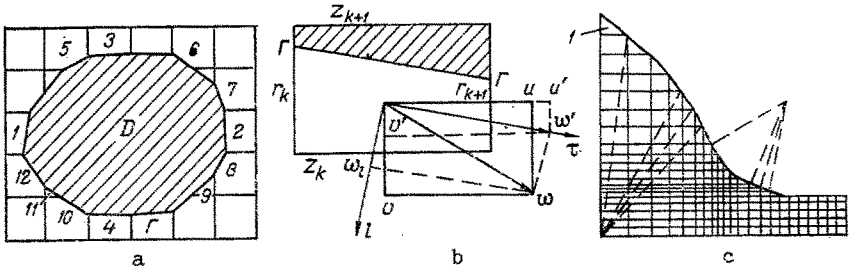

Fig. 1. Examples of the approximation of curved boundaries on regular (a) and irregular (c) grids using fractional cells, in each of which the velocity vector can be reconstructed (b) in accordance with Eq. (1).

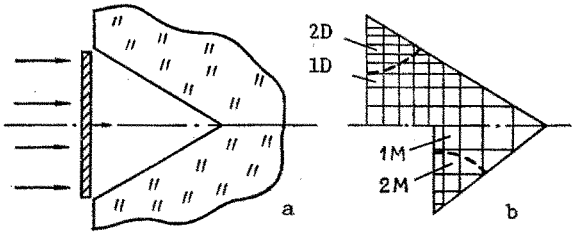

Fig. 2. Diagrams of loading of a conical cavity by a plate (a) and of the variation of the calculating grid in this cavity at different times (b). Regions of one-dimensional (1D) and two-dimensional (2D) flow are separated by a dashed curve.

$$X_{ij}^{n+1} = \tilde{X}_{ij}^{n} + A_{i-1/2}\begin{cases}\tilde{X}_{i-1,j}^{n}\tilde{u}_{i-1/2,j}^{n},\ \tilde{u}_{i-1/2,j}^{n} \geqslant 0\\ \tilde{X}_{ij}^{n}\tilde{u}_{i-1/2,j}^{n},\ \tilde{u}_{i-1/2,j}^{n} < 0\end{cases} - A_{i+1/2}\begin{cases}\tilde{X}_{ij}^{n}\tilde{u}_{i+1/2,j}^{n},\ \tilde{u}_{i+1/2,j}^{n} \geqslant 0\\ \tilde{X}_{i+1,j}^{n}\tilde{u}_{i+1/2,j}^{n},\ \tilde{u}_{i+1/2,j}^{n} < 0\end{cases} +$$

$$+ A_{j-1/2}\begin{cases}\tilde{X}_{i,j-1}^{n}\tilde{v}_{i,j-1/2}^{n},\ \tilde{v}_{i,j-1/2}^{n} \geqslant 0\\ \tilde{X}_{ij}^{n}\tilde{v}_{i,j-1/2}^{n},\ \tilde{v}_{i,j-1/2}^{n} < 0\end{cases} - A_{j+1/2}\begin{cases}\tilde{X}_{ij}^{n}\tilde{v}_{i,j+1/2}^{n},\ \tilde{v}_{i,j+1/2}^{n} \geqslant 0\\ \tilde{X}_{i,j+1}^{n}\tilde{v}_{i,j+1/2}^{n},\ \tilde{v}_{i,j+1/2}^{n} < 0;\end{cases} \tag{4}$$

$$\tilde{X}^{n} = \{\rho^{n},\ \rho^{n}\tilde{u}^{n},\ \rho^{n}\tilde{v}^{n},\ \rho^{n}\tilde{E}^{n}\},$$

$$X^{n+1} = \{\rho^{n+1},\ \rho^{n+1}u,\ \rho^{n+1}v,\ \rho^{n+1}E^{n+1}\}.$$

In the whole cells $u_{ij}^{n+1} = u_{ij}$ and $v_{ij}^{n+1} = v_{ij}$, while in the fractional cells u_{ij}^{n+1} and v_{ij}^{n+1} are determined through u_{ij} and v_{ij} from Eqs. (1). The condition (2) is used in Eq. (4) to calculate E_{ij}^{n+1} for cells adjacent to the moving boundary.

In Eqs. (3) and (4) the following notation is adopted:

$$A = \frac{\Delta t}{2V_{ij}\rho_{ij}^{n}},\quad A_{i\pm1/2} = \frac{S_{i\pm1/2}\Delta t}{V_{ij}},\quad A_{j\pm1/2} = \frac{S_{j\pm1/2}\Delta t}{V_{ij}},$$

$$p_{i\pm1/2,j}^{n} = \frac{p_{i\pm1,j}^{n}\Delta z_i + p_{ij}^{n}\Delta z_{i\pm1}}{\Delta z_i + \Delta z_{i\pm1}},\quad p_{ij\pm1/2}^{n} = \frac{p_{i,j\pm1}^{n}\Delta r_j + p_{ij}^{n}\Delta r_{j\pm1}}{\Delta r_j + \Delta r_{j\pm1}}$$

$$u_{i\pm1/2,j}^{n} = \frac{u_{i\pm1,j}^{n}\Delta z_i + u_{ij}^{n}\Delta z_{i\pm1}}{\Delta z_i + \Delta z_{i\pm1}},$$

$$\tilde{v}_{i,j\pm1/2}^{n} = \frac{\tilde{v}_{i,j\pm1}^{n}\Delta r_j + \tilde{v}_{ij}^{n}\Delta r_{j\pm1}}{\Delta r_j + \Delta r_{j\pm1/2}}\ \text{etc.}$$

By analogy with [4, 6], the system of equations (3)-(4) is homogeneous and conservative for cells of any type, the condition of nonpenetration is satisfied automatically when the area of the lateral surface ($S_{i\pm1/2}$ or $S_{j\pm1/2}$) equal zero, coinciding as a whole with the surface of the body over which the flow occurs. In the case of a boundary with nonpenetration, instead of the equality of the area to zero one can take the pressure inside it as equal to the pressure p_{ij} in the cell being calculated.

For many axisymmetric problems the number of types of fractional cells can be reduced considerably by breaking up the curved boundary with an irregular orthogonal grid in such a way that all the boundary cells are triangular (Fig. 1c). Then only four types of fractional cells, differing in the location of the region occupied by the gas, are possible near the surface of the boundary. In this case any fractional cell is bounded by two whole cells and the linear dimensions of their contiguous sides are the same. In this case the computation algorithm hardly differs in complexity from that for calculations of whole cells, since problems of combining small cells, stability, and approximation disappear. The success of such an approach is indicated by examples of calculations of gasdynamic flows in an explosive plasma generator [5, 8] and a magnetoplasma compressor [9].

Examples of Calculations. Let us consider the compression of gas inside a conical cavity by a thin plate thrown in the direction of the apex of the cone (Fig. 2a). Such a scheme is sometimes used in experiments on controlled thermonuclear fusion [10, 11], where instead of a flat plate or striker compressing the gas, a striker in the shape of a spherical segment with a radius equal to the length of the generatrix of the cone is used. In our case the problem becomes two-dimensional, while the gasdynamic flow in the cavity has a more complicated structure than in the quasi-one-dimensional case [10, 11]. Let us consider certain peculiarities of the construction of the numerical algorithm due to the presence of curved and moving boundaries.

At $t = 0$ let the plate instantly acquire a velocity U^n and move into the cone by $U^n\Delta t$. In the process, the size of the first row of cells changes by $U^n\Delta t$, and the mass and radius of the plate also decrease due to its cutting off against the wall of the cone. The gasdynamic flows are calculated from Eqs. (1)-(4) with allowance for the new size of the cells, and in the second stage the movement of the gas due to its expulsion by the plate is taken into account. The pressure and temperature are found in accordance with the equation of state of the specific medium and the new velocity U^{n+1} of the plate is calculated from the law of its motion. With this the calculation of the time step is completed.

As the plate approaches the boundary of a cell of the Eulerian grid $\Delta z_1 \to 0$ and hence, in accordance with the Courant condition, $\Delta t \to 0$. Therefore, when $\Delta z_1 = z_{min}$ in the calculations, the procedure of combining cells of the row Δz_1 with those of the second row Δz_2 is carried out so that the volume of the cells of the new row equals the sum of the volume of cells of the two former rows (we note that three cells are combined into one near the junction of the plate with the generatrix of the cone). The values of the gasdynamic quantitites in each new combined cell are determined from the laws of conservation of mass, momentum, and total energy.

We note a number of peculiarities of the flow under consideration, which can have practical importance in the solution of other problems. If the plate moves at a supersonic velocity with respect to an initially stationary gas, then sections of one-dimensional and two-dimensional flows can be isolated in the calculation region (Fig. 2b). In the process of the calculations one can trace the propagation of a shock wave from the corner of the junction of the plate and the generatrix of the cone (in the r direction) and the departure of the direct wave from the plate (in the z direction). The number of cells in the calculation must be increased in accordance with the motion of these waves. This procedure enables one to achieve considerable savings of computation time and computer memory. For example, having a grid that grows from 3 × 3 to 20 × 20 cells, one can, by renumbering the nodes, run through a space of 100 × 100 cells. In this case the calculation accuracy is increased in accordance with Richtmyer's analogy [3, 12], according to which in a calculation on a finite-difference grid one models a process analogous to the real one, with viscosity effects here being dependent either on artificial or schematic viscosity, while cells of the grid play the role of the colliding particles. In the above-indicated example there are an average of 10 cells along each coordinate in the calculation, enabling one to achieve ∿10 "collisions" and assure good resolution of the flow structure.

TABLE 1. Comparison of Results of Test Calculations of the Problem of Loading of a Conical Cavity by a Flat Piston (in a grid of 50 × 50 cells) with Allowance for Eqs. (1) and with Different Boundary Conditions at the Plate (a, b)

t·0.1, μsec	Number of cells passed through by the plate	$\Delta E_{ij} = \sum_i p_{ij} \Delta V_{ij}$ (a)					Eq. (4) (b)				
		E, kJ	U	u_{11}	v_{ph}	v	E, kJ	U	u_{11}	v_{ph}	v
			km/sec					km/sec			
0,2	3	$2,98 \cdot 10^{-7}$	60,00	0,08	—34,59	—1,91	$9,32 \cdot 10^{-5}$	59,93	51,55	—34,59	—32,93
0,8	14	$1,69 \cdot 10^{-4}$	58,82	1,68	—33,96	—25,82	$4,00 \cdot 10^{-4}$	58,71	58,48	—33,90	—33,93
1,4	23	$6,12 \cdot 10^{-4}$	53,86	19,72	—31,09	—34,24	$6,55 \cdot 10^{-4}$	55,96	54,85	—32,31	—32,86
2,0	32	$8,49 \cdot 10^{-4}$	48,10	40,89	—27,77	—29,78	$8,35 \cdot 10^{-4}$	50,94	51,60	—29,41	—29,86
2,4	38	$9,31 \cdot 10^{-4}$	43,07	42,58	—24,87	—26,34	$9,26 \cdot 10^{-4}$	44,19	45,18	—25,51	—26,43

TABLE 2. Comparison of Results of Test Calculations of the Problem of Loading of a Hemispherical Cavity by a Flat Piston (in a grid of 25 × 25 cells) with Allowance for Eqs. (4) and without (a) and with (b) Allowance for (1)

t, μsec	No. of cells passed through by the plate	a					b				
		E, kJ	U	u_{11}	v_{ph}	v	E, kJ	U	u_{11}	v_{ph}	v
			km/sec					km/sec			
8,0	3	1,92	5,084	4,520	—2,729	—2,433	1,92	5,084	4,521	—2,729	—2,608
10	9	5,93	5,402	5,379	—4,835	—4,623	5,92	5,402	5,380	—4,835	—4,817
11	13	10,12	5,462	5,392	—7,172	—6,258	10,15	5,463	5,392	—7,174	—6,678
12	17	21,32	5,359	5,384	—10,79	—9,157	21,43	5,363	5,387	—10,80	—9,986
12,5	20	38,76	4,793	4,990	—14,54	—12,13	38,84	4,811	5,003	—14,59	—12,97

The convergence of the numerical solution to the exact one on different finite-difference grids was studied in test calculations. In the case of the "standard" condition at the moving boundary (equality of the velocities of the gas and the plate) it was found that when the plate moves with a constant velocity, good agreement between the calculated and exact values of the gasdynamic variables behind the front of the developing plane shock wave is achieved only when the plate passes through 30-50 cells. In this case the separation of the front from the piston is 3-30 cells, depending on the intensity of the shock wave and the thermodynamic properties of the gas. From this it is seen that to achieve satisfactory accuracy in the description of gas flow only in the initial stage of motion of the plate requires a grid having 40-80 cells along each axis, i.e., close to the practical limit usually used in two-dimensional calculations.

The use of (2) in the energy equation in the second stage enables one to achieve considerable improvement of the convergence. Satisfactory agreement between the mass velocity u_{11} of the gas in the cell in front of the plate and the plate velocity U is observed when it has passed through only 5-10 cells (under the condition that the plate passes through each cell in no less than 100 time steps). The difference in the total amounts of energy E acquired by the gas at the end of the compression in cases a and b (Table 1) is a maximum of several percent.

The problem of the motion of a plate in a gas-filled cavity discussed here has a characteristic physical peculiarity: The main energy input into the gas and its acceleration are determined by the phase velocity of motion of the line of junction of the piston with the side wall. In this case the calculation accuracy is determined by how the finite-difference "flow" develops within the angle formed by the plate and the walls of the cavity. As is seen from Table 1, the use of (2) enables one to obtain good agreement between the radial components of the mass velocity v and the phase velocity v_{ph} ($w_{ph} = U/\sin\beta$) already in 5-10 cells. Satisfactory equality of these velocities in calculations on a grid twice as fine is also achieved in the case when the phase velocity is not constant but grows due to the decrease in the angle β (inside a hemispherical cavity), with the use of Eqs. (1) yielding somewhat more precise results, as is seen from Table 2.

Thus, the data presented indicate that the boundary conditions under consideration enable one to improve the accuracy and convergence of calculations on a more economical grid. The effect of the use of (2) is such that only with its help did it become possible in practice to obtain a satisfactory result on grids of 2000-3000 cells. The condition (1) is realized not at the boundary but inside a fractional cell. This seems problematical at first glance, especially for the first corner cell (see 1 in Fig. 1c), in which one side moves while the other deflects the stream. Here it should be noted that the slippage condition does not alter but only supplements the usual conditions of nonpenetration (or partial penetration) in a fractional cell, determined at its sides, as usual. Inside a corner (two of them in a cone: at the plate and at the apex), orientation of the vector along the lateral surface means the simultaneous orientation of the velocity components (v and u) along the other direction (the r and z axes, respectively). As the calculations show, this improves the accuracy. A similar effect is achieved not only for triangular cells but also for the arbitrary fractional cells considered in [7].

A qualitative picture of the development with time of the shock-wave flow inside conical and hemispherical cavities is shown in Fig. 3. Two shock waves are formed at the start of the motion of the plate in the cone (Fig. 3a): a direct one (1) and a refraction wave (2). Their mutual intersection can lead to the formation of a triple configuration (of the Mach type) and the appearance of wave 3 (Fig. 3b). These shock waves undergo a number of reflections, as a result of which wave 1 disappears (Fig. 3c, d). Inside a spherical segment the shock-wave pattern, initially also consisting of waves 1 and 2 (Fig. 3e), evolves somewhat differently. Here the appearance of wave 3 (Fig. 3f) is due to the reflection of wave 1 on the wall of the segment, since the line of junction of the front of wave 1 with the wall surface moves with a higher phase velocity than the line of junction of this surface with the front of wave 2. As the plate approaches the apex of the segment, the phase velocity grows rapidly and the gasdynamic flow takes on a cumulative character, manifested in the development of high-energy radial jets. Then after the collapse of these jets, moving behind the front of wave 2, a dense compact cluster is formed at the axis of symmetry (Fig. 3g, h), where the parameters of the gas reach the maximum values. We note that at the intersections of the fronts of waves 2 and 3 (Fig. 3c, d, f, g) the formation of triple configurations is possible, but special conditions are probably required for this (e.g., a large radius of

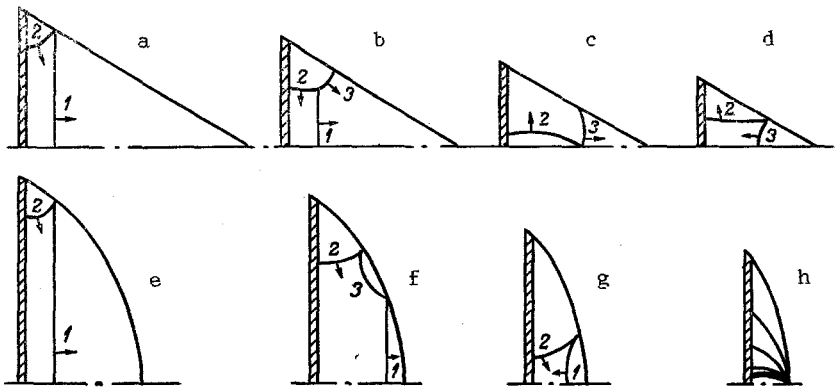

Fig. 3. Qualitative picture of the evolution of shock waves inside a cone and a hemisphere. The plate is hatched.

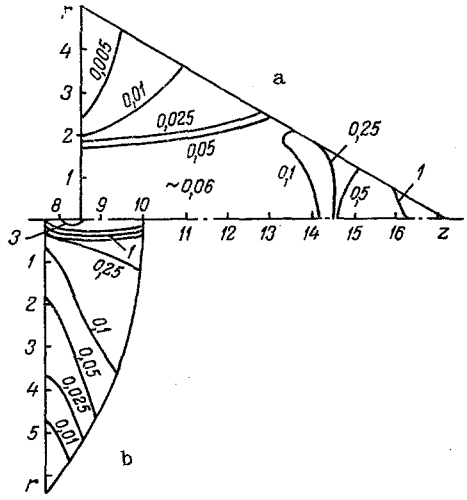

Fig. 4. Spatial distribution of isobars (Mbar) in conical (a) and hemispherical (b) compression chambers; r, z, cm.

curvature of the spherical segment, the conditions determining the aperture half-angle of the cone and the plate velocity, etc.). In the variants of the calculations discussed, the same shock-wave pattern as in Fig. 3 was obtained.

For a quantitative comparison of the parameters of the maximum compression inside conical and hemispherical targets of aluminum filled with deuterium initially at 1 atm, we made calculations of variants of loading of the cavity by a plate with a thickness of 0.01 mm, a density of 1.3 g/cm^3, and a diameter of 2 mm. Initially having a velocity of 60 km/sec, the plate moved into a cone with an angle of 60° at the apex or a hemisphere with a diameter of 2 mm and was decelerated, losing its kinetic energy through the decrease in area and the work performed on the gas. Radiative transfer and vaporization of the walls were taken into account in the problem by analogy with [8]; the processes of acceleration of the plate and the deformation of it and the walls were not considered. The thermodynamic properties of the deuterium plasma were assigned from a table constructed on the basis of the data of [13] and calculations from the Saha model.

In the conical target the maximum parameters p = 1.1 Mbar, ρ = 0.11 g/cm^3, and T = 22 eV are reached behind the reflected shock wave 3 (Fig. 4a) when the flow structure corresponds to the pattern shown in Fig. 3d. The velocity of the plate at this instant is 6.1 km/sec. Inside the spherical segment the maximum of the gasdynamic quantities (p = 3.1 Mbar, ρ = 0.12 g/cm^3, T = 28 eV) lies in a narrow layer at the axis of symmetry at the instant the plate fully stops (Fig. 4b). As we see, the extremal parameters are comparatively close in the

cases of the two targets. The calculations of these problems were made on a grid of 50 × 50 cells and the calculation time was about 1 h on a BÉSM-6 computer.

In conclusion, we note that the quantitative values of the gasdynamic quantities in the problems under consideration depend strongly on the precise description of the sections of flow near the junction of the plate and the walls of the compression chamber, as well as at the apex of the cone or the spherical segment. The most careful possible observance of the conditions of stream slippage along the curved surface at each point of it is required here.

NOTATION

T, temperature; p, pressure; E, total specific energy; ρ, density; $\mathbf{w}$, vector of mass velocity of the gas; u, v, axial and radial velocity components; z, r, axial and radial coordinates; t, time; U, velocity of the plate; ΔT, ΔZ, ΔR, steps in time and space; S, V, area of the lateral surface and volume of a cell; z_{min}, minimum size of a cell of the grid along the z axis; β, angle of junction of the plate and the compression chamber. Indices: i, j, centers of cells of the grid along z and r; k, fractional cell; ph, phase velocity, n, number of the time step; ($\sim$), intermediate values of gasdynamic quantities.

LITERATURE CITED

1. J. F. Thompson, Z. U. A. Warsi, and C. W. Mastin, "Boundary-fitted coordinate systems for numerical solution of partial differential equations (review)," J. Comput. Phys., 47, 1-108 (1982).
2. Numerical Grid Generation, J. F. Thompson (ed.), Proceedings of Symposium on Curvilinear Coordinate Systems and their Use in the Numerical Solution of Partial Differential Equations, Nashville, Tenn. (1982), Appl. Math. Comput., 10-11, 1-863 (1982).
3. P. J. Roache, Computational Hydrodynamics, Hermosa (1976).
4. O. M. Belotserkovskii and Yu. M. Davydov, The Method of Large Particles in Gas Dynamics [in Russian], Nauka, Moscow (1982).
5. G. S. Romanov and V. V. Urban, "Numerical modeling of an explosive plasma generator in a gas-dynamic approximation," Inzh.-Fiz. Zh., 37, No. 5, 859-867 (1979).
6. B. P. Gerasimov and S. A. Semushin, "Calculation of flow over bodies of changing shape on a moving Eulerian grid," Differents. Uravn., 17, No. 7, 1214-1221 (1981).
7. Yu. M. Davydov, V. D. Kulikov, and E. V. Maiorskii, "Investigation of flow over working blade rows of the profiles of steam turbines by the method of large particles," Zh. Prikl. Mekh. Tekh. Fiz., No. 3, 47-50 (1984).
8. G. S. Romanov and V. V. Urban, "Numerical modeling of an explosive plasma generator with allowance for radiative energy transfer and wall vaporization," Inzh.-Fiz. Zh., 43, No. 6, 1012-1020 (1982).
9. S. I. Ananin and T. A. Lepshei, "Numerical modeling of the dynamics of plasma compression streams by the method of large particles," Dokl. Akad. Nauk, SSR, 27, No. 8, 710-713 (1983).
10. S. L. Bogolyubskii, B. P. Gerasimov, V. I. Liksonov, et al., "Yield of thermonuclear neutrons from a plasma compressed by an envelope," Pis'ma Zh. Eksp. Teor. Fiz., 24, No. 4, 206-209 (1976).
11. S. I. Anisimov, V. I. Vovchenko, A. S. Goncharov, et al., "Processes of generation of thermonuclear neutrons during laser action on a conical target," Pis'ma Zh. Tekh. Fiz., 4, No. 7, 388-392 (1978).
12. R. D. Richtmyer and K. W. Morton, Difference Methods of Initial-Value Problems, 2nd ed., Interscience, New York (1967).
13. V. P. Kopyshev and V. V. Khrustalev, "Equation of state of hydrogen up to 10 Mbar," Zh. Prikl. Mekh. Tekh. Fiz., No. 1, 122-127 (1980).